Efficient organic light-emitting diodes using polycrystalline silicon thin films as semitransparent anode

X. L. Zhu, J. X. Sun, H. J. Peng, Z. G. Meng, M. Wong, and H. S. Kwok
Center for Display Research and Department of Electrical and Electronic Engineering, Hong Kong University of Science and Technology, Clear Water Bay, Hong Kong, People's Republic of China

(Received 14 March 2005; accepted 5 July 2005; published online 17 August 2005)

Polycrystalline silicon (*p*-Si) is a good material for the construction of thin-film transistors (TFT). It is used for fabricating active-matrix organic light-emitting diode (AMOLED) displays. In this letter, we propose and demonstrate the application of boron-doped *p*-Si as a semi-transparent anode in making different color OLEDs. Without removing the ultrathin native oxide on the *p*-Si surface and employing *p*-doped hole transport layer to enhance holes injection, these OLEDs show comparable or even better performance to conventional OLEDs which use ITO as anodes. The present technique has the advantage of less masking steps in making AMOLED. © *2005 American Institute of Physics*. [DOI: 10.1063/1.2032604]

Organic light-emitting diodes (OLED) have attracted much interest due to their potential application in flat panel displays.[1–3] Conventional bottom emitting OLED always uses conductive indium tin oxide (ITO) as the transparent anode. Some other metal oxides such as aluminum-doped zinc oxide,[4] zinc-doped indium oxide[5] have been also tried as the anode. As for top-emitting OLED, many high work function metals such as Ag and Pt[6,7] have been studied as the anode material. *P*-doped Si has also been used in conjunction with silicon microdisplay OLED.[8,9] However, silicon has high absorption in the visible light which greatly reduces the performance of the OLED.

Active-matrix OLED requires the use of polycrystalline silicon (*p*-Si) to make thin film transistors (TFT).[10–15] In most designs, the *p*-Si in the pixel area is etched away and ITO is sputtered to form the anode. Since *p*-Si has low absorption in the visible spectrum range, it is worth exploring the use of *p*-Si as the conductive transparent anode. In this paper, we report OLEDs using *p*-Si as the anode for a bottom emitting device. Red, green, blue (RGB) OLEDs have been fabricated successfully. These OLEDs showed good electroluminescent (EL) characteristics in comparison with devices using ITO as the anode. With *p*-Si as the anode, fewer processing steps and fewer masks are required in fabricating AMOLED. This will present considerable savings and increase in production yield in manufacturing AMOLED devices.

The *p*-Si anode used in the present study is made by the process of metal-induced-crystallization (MIC). However, other types of *p*-Si, in particular, laser annealed *p*-Si, should work as well. The MIC *p*-Si was fabricated as follows. First low pressure chemical vapor deposition (LPCVD) was used to deposit 100 nm of low temperature oxide (LTO) on a Corning 1737 glass substrate. It was then followed by LPCVD of 50 nm of *a*-Si. Then nickel was sputtered onto the *a*-Si and annealed to give the MIC *p*-Si. Finally, boron ions at the dose of 4×10^{15} cm^{-3} were implanted at 40 keV into the MIC *p*-Si. The thickness and doping concentration of the *p*-Si used in the present experiments are exactly the same as the active layer for a *p*-Si TFT. This is to ensure that in the actual application of the present results to AMOLED, there is no need for an extra mask for making the anode of the OLED. In fact, the drain of the TFT and the anode of the OLED can be a continuous layer.

The sheet resistance of this *p*-Si was measured by four point Kelvin-probes to be ~200 Ω/□. This is somewhat higher than an ITO anode. However, since the holes only have to travel a short distance, the higher resistivity is tolerable. There was about 2–3 nm of native oxide on top of the *p*-Si. This oxide layer could in principle be used to block the diffusion of boron into the organic layer.[16] The conventional OLEDs were fabricated on commercial ITO coated glass with a sheet resistance of 25 Ω/□. There is no special treatment of the ITO as well as the *p*-Si substrate prior to deposition of the organic layers. It is because with the use of *p*-doped organic materials as the hole injection layers (HIL), better performance can be achieved as compared with treated ITO.[17]

4,4′,4″-tris(*N*-3-methylphenyl-*N*-phenyl-amino)-triphenylamine (*m*-MTDATA) doped with 2,3,5,6-tetrafluoro-7,7,8,8-tetracyano-quinodimethane (F_4-TCNQ) (2 mol %) were used as hole injection and transport layers (HTL) to enhance holes injection. 4,4-bis[*N*-(1-naphthyl)-*N*-phenyl-amino] biphenyl (NPB) served as interlayer following *p*-doped HTL. Tris-(8-hydroxyquinoline) aluminum (Alq_3) was used as the emitting layer as well as the electron transport layer (ETL) for green OLEDs. Alq_3 doped with 1.5 wt % 4-(dicyanomethylene)-2–t–butyl-6-(1,1,7,7,-tetramethyljulolidin -3-methoxy-4-y1-viny1)-4H-pyran (DCJTB derivative) and 3-tert-butyl-9,10-di (naphtha-2–yl) anthracene (TBADN) doped with 2 wt % 2,5,8,11-tert-tertbutylperylene (TBPe) were used as the red-emitting and blue-emitting layers, respectively. 2,2′,2″-(1,3,5-benzinetriyl) tris(1-phenyl-1-H-benzimidazole) (TPBi) served as the hole blocking layer and ETL. We utilized Li*F*/Al bilayer as the efficient electron injection cathode. Doping was achieved by co-evaporation of the two materials in different sources and the evaporation rate was monitored by two independent quartz crystal oscillators. The typical deposition rate was 0.1–0.2 nm/s, 0.2–0.4 nm/s and 0.02–0.03 nm/s for organic materials except for the dopant, metal, and LiF, respectively.

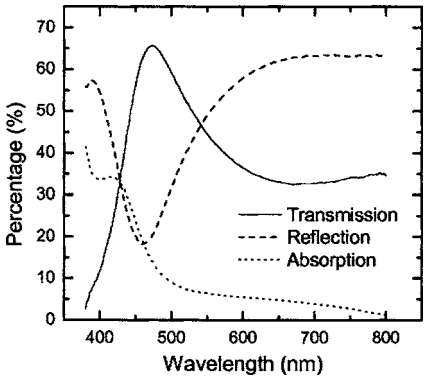

FIG. 1. Optical transmission, reflection, absorption of glass/LTO/MIC *p*-Si.

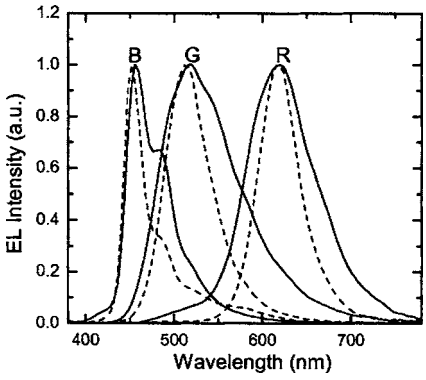

FIG. 2. EL spectra of red, green, and blue OLEDs from ITO (solid line) and MIC *p*-Si (dashed line) substrates in the normal direction.

Three types of OLEDs were fabricated in this study:

Type I: ITO (or *p*-Si)/m_MTDATA:F_4_TCNQ(2 mol %) ×(50 nm)/NPB(20 nm)/ Alq_3:DCJTB(1.5 wt %) ×(30 nm)/Alq_3(20 nm)/LiF(1 nm)/Al

Type II: ITO (or *p*-Si)/m_MTDATA:F_4_TCNQ(2 mol %) ×(50 nm)/NPB(10 nm)/ Alq_3(50 nm)/LiF(1 nm)/Al

Type III: ITO (or *p*-Si)/m_MTDATA:F_4_TCNQ(2 mol %) ×(40 nm)/NPB(10 nm)/ TBADN:TBPe(2 wt %) ×(20 nm)/TPBi(20 nm)/LiF(1 nm)/Al

Types I, II, and III are red, green, blue emitting devices, respectively. The current density-voltage (J-V) and luminance-voltage (L-V) characteristics of these devices were measured simultaneously with parameter analyzer (HP4145B) and a silicon photodiode calibrated by Photoresearch PR650 spectrometer. The EL spectra were measured with the PR650.

The optical transmission, reflection and absorption spectra of glass/LTO/MIC *p*-Si are shown in Fig. 1. Obviously the optical properties of the substrate will greatly affect the emission characteristics of the OLED devices. It can be seen that the MIC is relatively transparent throughout most of the visible spectrum, varying from 60% in the blue to 35% in the red. This reflectivity will affect the microcavity effect in the OLED. This variation has to be taken into account and compensated in designing full color RGB devices.

Experimental results of RGB OLEDs are summarized and listed in Table I. There are slight differences in the CIE chromaticity coordinates of the EL spectra from ITO and *p*-Si substrates. This is believed to be caused by the microcavity effect in *p*-Si devices. The exact emission peaks of the *p*-Si devices can be easily tuned by changing the thicknesses of the various components.[18,19] Figure 2 shows the EL spectra of the ITO and *p*-Si OLEDs in the normal direction. It can be seen that in general, the EL spectra of devices with *p*-Si as the substrate are sharper and narrower than those made with ITO. Again, this observation can be attributed to the microcavity effects caused by the strong reflection (~20% at λ=450 nm; ~49% at λ=550 nm; ~62% at λ=650 nm) of the semitransparent *p*-Si anode in the visible spectrum range.[6,20] The strong microcavity effects in *p*-Si based OLEDs also lead to angular variation of the emission spectra. Figure 3 shows the emission spectra of *p*-Si OLED at various viewing angles. It can be seen that there is some color shift due to the microcavity effect. It should be noted that we have not made any attempt to optimize the microcavity effect in terms of efficiency or the color variation in this preliminary investigation. Presumably the angular variation of the emission color can be minimized or even eliminated by optimizing the thicknesses of the various layers in the devices without compromising the performance of the device.[6,18,21]

Table I shows the normal-direction luminance efficiency of the various devices. It can be seen that the red and green OLEDs with *p*-Si anode are much more efficient than those using ITO as anodes. This is due to the strong microcavity effects leading to normal direction emission enhancement, as well as due to the lower absorption of the *p*-Si substrate at 520 nm (~7.5%) and at 620 nm (~5.3%). As for the blue OLEDs, the *p*-Si substrate device is less efficient than that of ITO substrate. This is probably due to the much larger absorption of the *p*-Si substrate at 456 nm (~21%).

TABLE I. Performance of RGB emitting OLEDs with ITO and *p*-Si anode.

Structures	CIE (x,y) (Normal direction)	Turn on voltage (V) at 1 cd/m^2	Voltage (V) at 20 mA/cm^2	Maximum luminance efficiency (cd/A)
Type I: ITO	(0.577 0.410)	3.6	7.8	3.75
p-Si	(0.631 0.365)	3.5	9.3	5.88
Type II: ITO	(0.300 0.529)	2.5	4.7	3.05
p-Si	(0.211 0.584)	2.6	7.8	3.67
Type III: ITO	(0.148 0.161)	4.0	10.2	2.44
p-Si	(0.173 0.144)	4.4	12.8	1.88

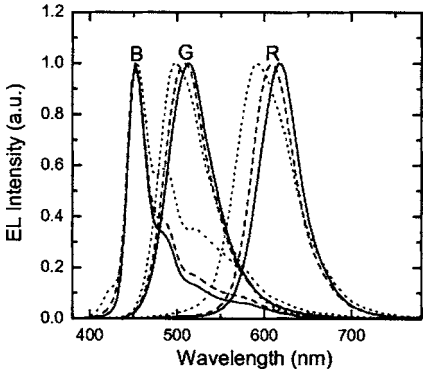

FIG. 3. EL spectra of red, green, and blue OLEDs on MIC *p*-Si at 0° (solid line), 30° (dashed line), 60° (dotted line) off the normal direction.

Also from Table I, we find that the ITO based and *p*-Si based devices of each type show similar turn-on voltages. It can be understood by the fact that the Fermi level of *p*-doped Si is ~4.7 eV, which is quite close to the work function of untreated ITO. However, due to the very large series resistance introduced by the larger sheet resistance of *p*-Si, the voltages required to achieve 20 mA/cm^2 for *p*-Si based devices are higher than those of corresponding ITO based OLEDs.

As an example, Fig. 4(a)–4(c) give the J-V, L-V, efficiency versus voltage characteristics of the red OLEDs, respectively. A brightness of 1,000 cd/m^2 can be obtained at 9.6 V with a luminance efficiency of 4.3 cd/A and power efficiency of 1.3 lm/W for the *p*-Si devices. Because of the higher series resistance, the current and brightness of the *p*-Si based device exhibits relatively slow increase, while the luminance and power efficiency are still much higher than those of the control ones.

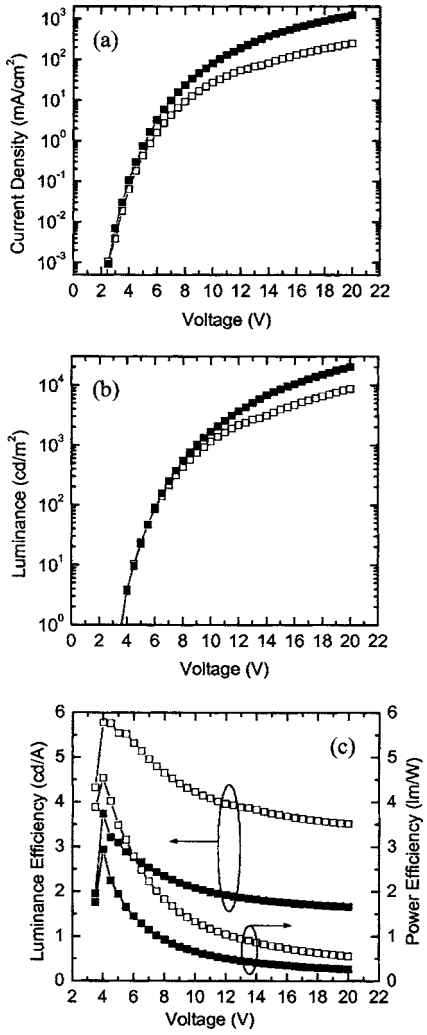

FIG. 4. (a) J-V, (b) L-V, and (c) luminance and power efficiency characteristics of red-emitting devices on ITO and MIC *p*-Si (■:ITO; □:MIC *p*-Si).

In summary, we have demonstrated RGB OLEDs using the boron doped MIC *p*-Si as the semitransparent anode. It is believed that other types of *p*-Si should show similar results. The emission and electrical characteristics of these devices have been analyzed and compared with the control ones using ITO anodes. Microcavity effects do exist due to the strong reflection of the semitransparent anode. However, using optimized device thicknesses, microcavity effects should not deteriorate the performance of these devices. On the contrary, microcavity effects can improve the performance, especially for red and green devices.

It is anticipated that *p*-Si is a good alternative anode to conventional ITO in AMOLED fabrication because an ITO mask can be eliminated. The OLED anode can be the same layer as the source and drain of the TFT in the pixel array, thus this device structure will result in a significant reduction of the number of processing steps. Simplification in processing should increase device yields and reduce manufacturing costs.

This research was supported by the Hong Kong Government Innovations and Technology Fund.

[1] C. W. Tang and S. A. Van Slyke, Appl. Phys. Lett. **51**, 913 (1987).
[2] J. Kido, M. Kimura, and K. Nagai, Science **267**, 1332 (1995).
[3] V. Bulović, P. Tian, P. E. Burrows, M. R. Gokhale, and S. R. Forrest, Appl. Phys. Lett. **70**, 2954 (1997).
[4] J. Zhao, S. Xie, S. Han, Z. Yang, L. Ye, and T. Yang, Synth. Met. **114**, 251 (2000).
[5] A. Yamamori, S. Hayashi, T. Koyama, and Y. Taniguchi, Appl. Phys. Lett. **78**, 3343 (2001).
[6] C. W. Chen, P. Y. Hsieh, H. H. Chiang, C. L. Lin, H. M. Wu, and C. C. Wu, Appl. Phys. Lett. **83**, 5127 (2003).
[7] C. F. Qiu, H. J. Peng, H. Y. Chen, Z. L. Xie, M. Wong, and H. S. Kwok, IEEE Trans. Electron Devices **51**, 1207 (2004).
[8] H. H. Kim, T. M. Miller, E. H. Westerwick, Y. O. Kim, E. W. Kwock, M. D. Morris, and M. Cerullo, J. Lightwave Technol. **12**, 2107 (1994).
[9] A. Aziz and K. L. Narasimhan, J. Appl. Phys. **88**, 4739 (2000).
[10] S. W. Lee and S. K. Joo, IEEE Electron Device Lett. **17**, 160 (1996).
[11] Z. H. Jin, H. S. Kwok, and M. Wong, IEEE Electron Device Lett. **20**, 167 (1999).
[12] D. Murley, N. Young, M. Trainor, and D. McCulloch, IEEE Trans. Electron Devices **48**, 1145 (2001).
[13] Y. G. Yoon, M. S. Kim, G. B. Kim, and S. K. Joo, IEEE Electron Device Lett. **24**, 649 (2003).
[14] M. Kimura, I. Yudasaka, S. Kanbe, H. Kobayashi, H. Kiguchi, S. Seki, S. Miyashita, T. Shimoda, T. Ozawa, K. Kitawada, T. Nakazawa, W. Miyazawa, and H. Ohshima, IEEE Trans. Electron Devices **46**, 2282 (1999).
[15] C. Wu, Z. Meng, J. Li, X. Zhang, G. Yang, S. Xiong, X. Shi, H. Peng, M. Wong, H. S. Kwok, S. Yin, D. Zhang, T. Sun, L. Wang, and Y. Qiu, Proc. S.I.D. 1128 (2004).
[16] K. W. Chan, C. H. Wan, H. S. Kwok, and M. Wong, Proceedings of the Sixth Chinese Optoelectronics Symposium, Hong Kong (IEEE, New York, 2003), p. 216.
[17] J. Huang, M. Pfeiffer, A. Werner, J. Blochwitz, K. Leo, and S. Liu, Appl. Phys. Lett. **80**, 139 (2002).
[18] H. Riel, S. Karg, T. Beierlein, W. Rieß, and K. Neyts, J. Appl. Phys. **94**, 5290 (2003).
[19] S. F. Hsu, C. C. Lee, S. W. Hwang, H. H. Chen, C. H. Chen, and A. T. Hu, Thin Solid Films **478**, 271 (2005).
[20] C. J. Lee, R. B. Pode, D. G. Moon, J. I. Han, N. H. Park, S. H. Baik, and S. S. Ju, Phys. Status Solidi A **201**(No. 5), 1022 (2004).
[21] C. C. Wu, C. L. Lin, P. Y. Hsieh, and H. H. Chiang, Appl. Phys. Lett. **84**, 3966 (2004).